Effectiveness of carbon polymeric nanofiltration composite membrane in treating industrial textile wastewater

Nouha Tahri[a],*, Michael O. Daramola[b], Raja Ben Amar[a],*

[a]*Chemistry Department, Faculty of Sciences of Sfax, University of Sfax, Road Soukra Km 4, 3000 Sfax, Tunisia, Tel. +216 21 064 024;
email: tahri.nouha@yahoo.fr (N. Tahri), Tel. +216 99 410 520; email: benamar.raja@yahoo.com/raja.rekik@fss.rnu.tn (R.B. Amar)*
[b]*Department of Chemical Engineering, Faculty of Engineering, Built Environment and Information Technology,
University of Pretoria, Hatfield 0028, Pretoria, South Africa, email: michael.daramola@up.ac.za*

ABSTRACT

Today, the trend is towards the use of low-cost materials to develop green processes in the aim to reduce cost and impact on environment. The use of low-cost materials of natural origin has been proven to be very promising for the fabrication of ceramic membranes for wastewater treatment. In this article, fabrication and testing of high performance microporous carbon membrane for nanofiltration (NF) separation based on mineral coal and phenolic resin are reported. The preparation of the NF composite membrane involved carbonizing a polymeric precursor deposited on a porous supported membrane, using the vacuum slip-casting process to obtain a homogeneous NF top layer almost without defects by one-step coating-carbonization cycle. To ensure a better final membrane texture, several parameters including the viscosity of the casting suspension, the casting time and the carbonization temperature were considered. A crack-free NF membrane with a thickness layer of 1.36 μm, a mean pore size of 1.1 nm, and a molecular weight cut-off of 400 Da was obtained using 1 min casting time and 45% of phenolic resin. These membranes were tested in the treatment of textile wastewater. Promising results in terms of permeate flux and pollutant retention (COD (72%), salinity (45%)) were obtained. The results further showed that the treated wastewater could be recycled into the textile industry or can be discharged into the municipal sewerage in compliance with legislations. In addition, a carbonization temperature of 650°C yielded best membranes in terms of average pores size and membrane permeability with minimum energy consumption.

Keywords: Composite polymeric nanofiltration membrane; Carbon; Vacuum slip-casting; Carbonization temperature; Textile wastewater

1. Introduction

Contamination and industrial development are among the reasons for water quality deterioration beyond treatability by conventional processes. The most of pollutants that are introduced significantly by many industries into the environment are organic in nature, such as detergents, drugs and dyes through the produced wastewater [1,2]. In general, the industrial effluents are loaded by different types of toxic substances which are stable and difficult to degrade due to their complex aromatic structure and synthetic origin [3]. Mittal et al. [4] reported that artificial dyes cause serious side effects, such as hyperactivity in children as well as cancer and allergies. Saharan et al. [5], found that the majority of dyes are water-soluble and have high or moderate toxicity, which can cause solemn damage to the living biota.

* Corresponding authors.

Membrane technology has emerged as a promising option in various processes and industrial sectors replacing conventional technologies due to their interesting features [2,6–10]. On the other hand, the increasing demand for highly efficient membrane separation process in terms of production and purity has resulted in increased global willingness to embrace membrane material as a potential long-term solution. Challenge for polymeric membranes such as limitations in selectivity and the low thermal and chemical resistance, even if they can be used at high pressures are no longer an issue for inorganic membranes. Inorganic membranes have a wide range of industrial applications for processing liquids. With the availability of the large number of inorganic materials, this field of research becomes attractive as a means to solving separation problems [11]. Inorganic membranes have a very wide range of pore sizes from microfiltration to reverse osmosis ranges depending on the materials of choice and synthesis conditions. Nanofiltration (NF) is a pressure-driven separation process, intermediate between reverse osmosis (RO) and ultrafiltration (UF), rejecting molecules having the size in the order of one nanometer [12–14]. Advantages of NF over RO include low operating pressure, relatively low investment, low maintenance costs, high water fluxes, high rejection of divalent ions and low rejection of monovalent ions [15–18]. These properties have allowed NF to be used in various applications in many areas, especially for water and wastewater treatment, pharmaceutical, biotechnology, and food engineering [19–22].

In addition to high chemical, thermal and mechanical stability of the pure inorganic NF membranes, other advantages of inorganic NF over polymeric membranes are reduction in fouling, easy regeneration and long service life. However, ceramic membranes are difficult to fabricate and may have many defects in the microstructure which require several additional steps avoid. For efficient NF for water purification application, NF membranes must be thin with narrow pore size distribution that assures high selectivity and permeability [23]. Depending on the nature of the material, inorganic membranes can be fabricated in thin film and multi-layer supporting structures with adequately strong and permeable characteristics [15,24]. Recently, the preparation of low-cost ceramic membranes with composition mainly based on natural materials (with the cost more similar to that of polymeric membranes) has encouraged the development of ceramic membranes at larger scale [25–28].

The innovation that combines the unique features of both polymeric matrix and inorganic fillers (otherwise known as mixed matrix membranes) has emerged as a promising solution for the above-mentioned shortcomings of inorganic NF membranes [29]. So, to overcome these problems and improve the performances of inorganic NF membranes, numerous studies have focused on the production of organic-inorganic composite membranes that combine characteristics of polymers and ceramics. For example, polymer infused with carbon nanotubes [30] or zeolite materials [31] or FeNPs [32] have been developed and tested for wastewater treatment. The polymer/ceramic composite membranes are potentially the most suitable for nanofiltration, gas separation and membrane distillation [33–35].

One material of interest in this field is carbon derived membranes which have been extensively developed for gas separation and investigated for liquid separation [36]. An advantage of carbon membranes is related to the good chemical and thermal stability due to the carbon structure of the membrane. In addition, the pore dimension of carbon membranes can be finely adjusted by thermo-chemical treatment (pyrolysis or carbonization) to give narrow pore size distributions. Temperature and the nature of the polymer precursor used during the production play an important role in the porosity formation [11]. Recently, carbon membranes fabricated from various carbonaceous materials have received great attention in many industrial areas. Of recent, tubular carbon membrane derived from coal has been successfully synthesized and tested in our laboratory [37–40]. Following this study, considerable efforts have been made in terms of developing precursors with low cost and high carbon yield, a good choice of the supported membrane and the preparation process, in order to reduce the cost of production and thus, obtain final material having good membrane quality [41]. Several parameters can affect the microstructure formation of the active layer, but the nature of the polymer precursor remains the crucial parameter that affects the final structure of carbon NF membranes [41,42]. Many researchers have employed phenolic resin and claimed that it is an excellent carbonaceous material for the preparation of microporous and nanoporous carbon layers due to its considerable fixed-carbon yield, high inherent purity and low cost.

NF carbon membranes are prepared by carbonization of a thin film of phenolic resin deposited on the inner face of a supported membrane. The traditional slip-casting (TSC) method is the most used method to deposit layers inside tubular supports. It has been shown that the TSC is an efficient process, which has been adapted mainly for the deposition of MF and UF layers [37,38,45,46]. It has been demonstrated that this approach allows the production of microstructure with fewer defects compared to other processes described in the literature [43,44]. The presence of these defects is probably because the precursor hardly penetrates into the pores of the substrate and cracks form during the pyrolysis which requires many repetitive casting-carbonization cycle to obtain a homogenous layer. In recent years, several research studies have highlighted the use of the vacuum slip-casting process (VSC: Vacuum Slip-Casting) as a solution to facilitate the working protocol and obtain a homogeneous layer almost without defects in one step. The VSC technique is based on the principle as that of the TSC process with the application of vacuum to have a uniform coating layer. This method is mainly adapted to produce NF membranes and dense membranes.

Many researchers have been focused on the application of NF carbon membranes for gas separation. Nevertheless, these membranes have great potential to be used in different areas under aggressive conditions thanks to their properties of chemical and thermal resistances. Currently, the application of carbon membrane to the liquid/aqueous solution separation is discussed by only a few researchers [42].

In this context and to contribute to scientific aspect in this area, the aim of this work is to present the synthesis

of low-cost composite carbon NF membrane and its application in the treatment and recycling of industrial textile wastewater.

2. Experimental

2.1. Preparation of NF carbon membrane

The composite carbon NF membrane was prepared by carbonizing thin film of phenolic resin deposited on the inner face of a porous support. Previous works in this field showed that the texture of the active layer is strongly influenced by the structural properties of the supported membrane since the defects of substrate will be translated to the top separative layer. It was also proved that depositing one or two intermediate layers between the macroporous support and the top layer should be essential to decrease or even avoid the risks of defects formation so as to ensure the success of membrane fabrication [38,48,49]. In this study, microfiltration (MF) carbon membrane has been used as a support for the NF top layer. The macroporous carbon tube (OD/ID = 10 mm/8 mm) having a pore volume of 38% and a mean pore diameter of 9 µm was prepared by extrusion–carbonization process. The intermediate MF layer with an average pore diameter of 0.6 µm and a thickness of 22 µm was obtained by slip-casting process followed by a curing–carbonization cycle at 700°C under a nitrogen flow of 1 mL/min. The method of preparation of these carbon-supported membranes has been described elsewhere [37,38].

The selective NF layer was prepared from a commercial Novolac-type phenolic resin purchased from Irons Resins S.A., Spain (Sumitomo Bakelite co).The phenolic resin was gradually dissolved in organic solvent (ethanol in this study) for 3–4 h. A complete dissolution and homogenization of the suspension was achieved to avoid agglomeration of the very fine particles of resin during the casting step. The suspension was then deposited in the inner surface of the supported substrate by the vacuum slip-casting (VSC) process: the supported membrane is enclosed in a module, putted vertically, connected to both ends with non-porous pipes and sealed with mastic As soon as this slip comes into contact with the porous tube, a vacuum is applied resulting in a pressure gradient allowing a deeper penetration of the suspension into the pores which improves the adhesion of the active layer and ensure a uniform distribution of the suspension over the entire inner surface of the tube (Fig. 1) [47].

It should be noticed that the control of the pump speed as well as the casting time is very important to avoid the damage of the Plexiglas module and then the membrane. Indeed, under a high pressure, a strong absorption of the suspension by the pores can be happen leading to the blockage of the pores. The sealing between the Plexiglas module and the pipes must be well checked to avoid the flow of the suspension under pressure.

The membrane was then immediately cured in air at 150°C for 2 h (heating rate of 1°C/min) under continuous rotation inside an oven to assure uniformity of membrane thickness. The carbonization step was carried out in a quartz tube inside a tubular horizontal Termolab furnace
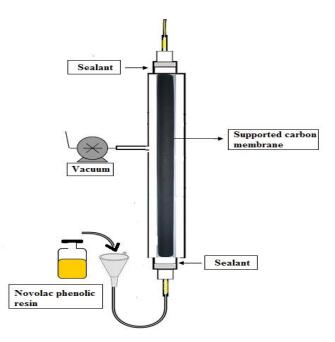

Fig. 1. Vacuum slip-casting device used for the preparation of NF top layer.

(VTF7 VECSTAR) using nitrogen atmosphere at flowing rate of approximately 1 mL/min.

2.2. Membrane characterization and separation performance evaluation

The average pore size and pore size distribution of the NF membrane were checked by nitrogen adsorption/desorption isotherm using a Micromeritics Asap 2010. Pore diameter was estimated by BJH (Barret–Joyner–Halenda) method [50].

A scanning electron microscopy (SEM) was used to observe the morphology of inner surface and cross-sectional surface of the obtained membrane. The molecular weight cut-off (MWCO) was determined using 1 g/L aqueous solution of various polyethylene glycol (PEG) molecules with molecular weight ranging from 2 to 300 kDa. The system was thoroughly rinsed with pure water between runs to check that membranes were not fouled during the cut-off determination.

Cross-flow filtration experiments were carried out with single channel tubular membrane having an active surface area of 13.6 cm². Before each run, the membrane was conditioned in ultrapure water with a resistivity of 18 M Ω cm for 24 h to get a fast stabilization of the permeate flux. Permeability was then obtained according to the Darcy's law in Eq. (1):

$$J_w = \frac{TMP}{\mu \cdot R_m} \tag{1}$$

where R_m is membrane resistance, μ is water viscosity and TMP is operating transmembrane pressure. The retention rate (R) was determined using the following classical relation:

$$R(\%) = 100 \times \left(1 - \left(C_p - C_f\right)\right) \qquad (2)$$

where C_p and C_f are the PEG solute concentrations in the permeate and in the feed solution, respectively.

3. Results and discussion

3.1. Preparation of carbon nanofiltration membrane

The NF layer was prepared by deposition of an alcoholic solution of phenolic resin type Novolac® (PR) on the inner face of the MF supported membrane. To ensure a better final membrane texture, the determination of the adequate suspension viscosity and the optimal casting time is indispensable. These parameters have a considerable effect on control of the layer thickness and consequently it influences defect formation. In order to determine the optimal viscosity, different layers with different percentages of phenolic resin (PR) were made. According to the literature, the PR concentration varies between 35% and 70% [48,51–53] (Table 1). The resin was dissolved progressively in the organic solvent, which is ethanol in this study, for almost 3–4 h until a complete dissolution in order to obtain a perfect homogeneity of the solution so to avoid the agglomeration of very fine particles of the resin during the casting operation.

In this study, the concentration of PR is limited to a percentage of 65% because beyond this value the solution is almost saturated with resin and the dissolution of the powder is very difficult. Samples codes were determined according to this form: $NF_{PR\,percentage}$ (Table 1).

Morphology of the surface and cross-section of the prepared membranes using the different casting times were characterized by SEM. It is noticed here that the SEM images are representative of the total analyzed surface by considering three samples taken from different locations on the tubular membrane. The microstructural study of the various samples shows an asymmetric structure composed of a macroporous substrate, an intermediate layer and almost a dense upper layer. It was also observed that the texture of the membrane surface as well as the thickness of the resulting layers evolve significantly with the viscosity of the suspension (Fig. 2). The suspension containing 65% of PR, whatever the casting time employed in the synthesis, led to the formation of cracked layers that exhibit poor adhesion to the membrane surface. Because of the high viscosity of the

slip (58cp), the solution crosses the wall of the membrane support without it being able to penetrate. After carbonization, the formed layer could not be held by the substrate and consequently it is completely taken off from its surface.

When analyzing the texture of surface of the other membrane, it was concluded that the majority of the formed layers obtained using a casting time of 60 s contained fewer defects (cracks and pinholes) than those obtained after casting duration of 30 and 9 0 s. It appears from Fig. 2, illustrating the micrographs of the NF layers realized at 60 s casting time and using the different composition, that the use of low concentration of PR (content varying between 35% and 45%) lead to a homogenous texture with fewer defects. It is clearly observed that concentration of 45% in PR leads to a perfectly smooth and practically defect-free layer. Beyond this value, defects tend to form. At a high concentration of 60%, the layer is completely damaged.

Furthermore, the thickness of the top layer plays an important role in defect formation as well as in separation properties [38]. In addition to the effect of the casting time on the quality of the as-prepared membranes, the viscosity of the precursor solution (related to the concentration of the PR) has a considerable influence on the thickness of the formed layers.

Fig. 3 shows that the thickness of the membrane layer increased almost linearly with the viscosity of the slip. For instance, a membrane thickness of 0.84 and 1.36 μm was recorded for the NF_{35} and NF_{45}, respectively. This could be attributed to the low viscosity of the suspensions (31cp (for NF_{35}) and 38cp (for NF_{45})). Increasing the PR concentration beyond these values resulted in formation of membranes with increased layer thickness of about 54% and 70% for the NF_{50} and NF_{55} membrane, respectively, and to reach a maximum value of 4.7 μm for NF_{55} layer. When the viscosity of the suspension is very high, the penetration of the precursor into the supported membrane will be more difficult which resulting in accumulation of the solution on the membrane surface and subsequently the formation of a thick layer. The proportional increase of the thickness of the layer with viscosity is accompanied with the formation of defects on the membrane surface and this explains the difficulty of detecting the thickness of the NF_{60} layer.

In conclusion, the slip with low viscosity (31cp) can cover easily the supported membrane and embrace all its irregularities, but it was not sufficient to maintain a homogeneous layer without defects (NF_{35}). Increasing resin concentration that does not exceed 45% greatly improves the surface texture of the membrane layer during casting time of 1 min. A thin, good quality layer was formed with a thickness that does not exceed 1.36 μm (Fig. 4). Good adhesion between NF layer and the supported membrane can be observed. Similar results have been reported by Briceno et al. [54]. In the report, the authors demonstrated that a good choice of the type of the polymer precursor as well as the use of low concentrations of the slip casting allows better penetration of the suspension in the pores of the supported membrane and subsequently the formation of regular layer that adhered well to the surface. In addition, the increase in viscosity (high polymer concentration) leads to the appearance of defects because of the thickness of the polymer film.

Table 1
Conditions tested for NF layers preparation

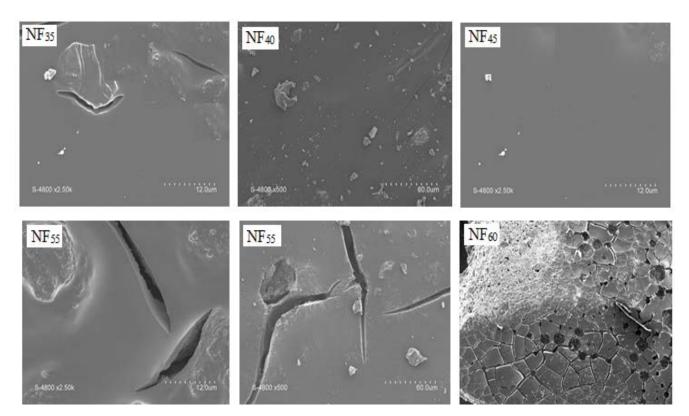| NF layer code	PR in alcoholic solution (wt.%)	Viscosity (cp)
NF_{35}	35	31
NF_{40}	40	34
NF_{45}	45	39
NF_{50}	50	42
NF_{55}	55	48
NF_{60}	60	53
NF_{65}	65	58

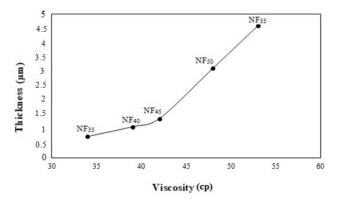Fig. 2. Evolution of the texture of NF layers based on PR content.

Fig. 3. Thickness of the NF layer as a function of the viscosity of the suspension at casting time of 1 min.

Thus, it could be concluded that NF membrane of good quality can be obtained by using 45% of PR in alcoholic solution for casting time of 1 min

3.2. Effect of carbonization temperature on the micro-porosity of the NF layer

Obtaining a defect-free thin layer film of carbon membrane is crucial as several parameters are considered. Besides the casting method, the heat treatment process, which includes temperature, heating rate, gas flow rate, environment gas, and soaking time, was responsible for the pore dimension adjustment of carbon membranes to give narrow pore size distributions [50,55,56].

Several studies have reported that the carbonization temperature of phenolic resin as thermosetting precursor has a remarkable effect on the microporous structure of the final material [44,53,57]. It has also been shown that optimizing the preparation conditions of the NF layer can significantly improve the performance of the final NF membrane. For this, to avoid membrane defects (e.g., cracks and pinholes) so as to maintain the membrane selectivity, in addition to the determination of deposition conditions, a study of the effect of the carbonization temperature on the structural characteristics of pores was carried out. The reticulated NF_{45} membranes, at 150°C, were carbonized under inert atmosphere using five different temperatures, 500°C, 600°C, 650°C, 700°C and 750°C with an increase of 1°C/min and a level of 2 h. The resulting membranes codes were used as follows: $NF_{45/Carbonization\ temperature}$.

N_2 adsorption-desorption analysis at 77 K was used to determine the effect of the carbonization temperature towards the carbon membrane layer by studying the BET surface area, total pore volume, micropore volume and average pore diameter. Fig. 5 shows that all the prepared samples carbonized at various carbonization temperatures (500°C–750°C) exhibit type I behavior according to IUPAC, which corresponds to a microporous structure. The adsorption equilibrium was established at a very low relative pressure and the slight gain in uptake at the end (p/p0 ~ 1) for carbonized membranes at 500°C and 600°C can be attributed to the presence of some mesopores or macropores in the structure of the active layer. Generally, the adsorbing side of the carbon membrane resulted from the existence of micropores which led to this isotherm adsorption types [58].
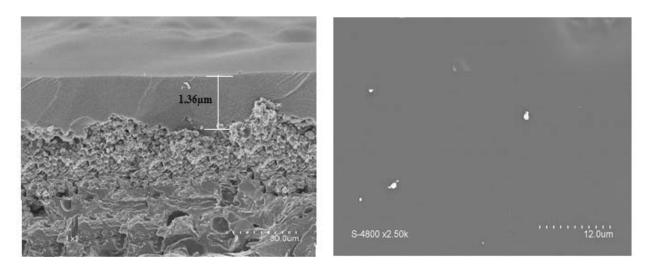
Fig. 4. Micrographs of the cross-section and surface of the optimized NF membrane.
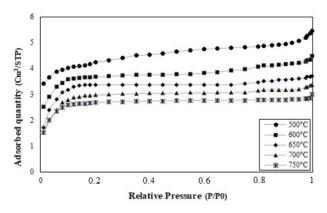

Fig. 5. N_2 adsorption isotherms of NF membranes carbonized at different temperatures.

Fig. 6. Average pore size of the NF_{45} membrane as a function of the carbonization temperatures.

The average pore diameter as well as the water permeability of NF membranes as a function of the carbonization temperature is depicted in Fig. 6. The increase in the carbonization temperature causes a decrease of the average pore size of 2 nm, obtained by carbonizing at 500°C, to stabilize at a value of about 1.1 nm with a temperature of 650°C which will influence permeability and membrane performance. It should be noted that water permeability is inversely proportional to the used carbonization temperature. There was a slight decrease of permeability from 9.87 to 7.6 L/h m² bar for membranes $UF_{45/500°C}$ and $UF_{45/650°C}$, respectively, followed by a brusque drop to a value of around 2.4 L/h m² bar obtained by the $UF_{45/750°C}$ membrane.

Centeno et al. [59] have reported, as well, that the increase of the carbonization temperature has led to a decrease of water permeability but the selectivity during the permeation of Helium gas increases considerably in a temperature area of 650°C–700°C. Some researchers [60–63] have concluded that the change in membrane selectivity with carbonization temperature is related to the modification of the textural properties of the selective layer. The pyrolysis of resin involves the development of pores at a temperature of about 450°C–500°C and its enlargement to a temperature of about 650°C. The use of higher temperatures
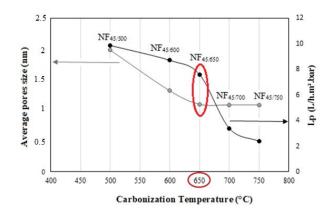
caused these pores to shrink, and they disappeared even at temperatures close to 1,000°C. To minimize the energy consumption and at the same time obtain a final material with the desired characteristics, the carbonization temperature of 650°C seems to be reasonable to prepare NF membranes from PR.

To determine the Molecular Weight cut-off (MWCO) of the prepared membrane, different molecular mass of PEG (1 g/L) solutions ranging from 100 to 2,000 Da were used. The retention rate of the polymer in solution was gradually increases with the PEG molecular weight and then stabilizes when 90% or more of the solute is retained by the membrane. The stabilized value is in the order of 400 Da (Fig. 6).

The conditions preparation as well as the characteristics of the optimized NF carbon membrane is illustrated in Table 2.

3.3. NF membrane performance testing

3.3.1. Wastewater origin and quality

The study was conducted with a real textile wastewater sample supplied from a Tunisian textile factory which specialized in the dyeing and washing processes.

Table 2
Conditions preparation and the characteristics of the optimized NF carbon membrane

Conditions of layer preparation			Characteristics of the optimized NF carbon membrane			
PR percentage (%)	Vacuum casting-time (min)	Carbonization temperature (°C)	Thickness (μm)	MWCO (Da)	Average pores size (nm)	Lp (L/h m² bar)
45		650	1.36	400	1.1	7.6

The generated wastewater, currently treated with activated sludge, is notorious for its recalcitrant characteristics including complex structures such as wetting agents, dyes, fixing agents, softeners and many other additives and it is not quite into compliance with the Tunisian standard of wastewater discharge to public sewers (Table 3).

3.3.2. Performances of application of NF membranes

The retention of organic and inorganic compound as well as the established fouling are sensitive to the changes in working conditions. In addition, the permeate flux and quality can be improved by adjusting the filtration conditions such as temperature, pressure and salinity.

The temperature used in this study was fixed at around 30°C to minimize the energetic costs. The choice of this temperature was based on other works [37,63–65] which was found that the effluent's quality and viscosity did not change with the temperature range of 25°C–50°C. Generally, the permeate flux increases very slightly with temperature in the case of textile wastewater and in the temperature range of 24°C–50°C, the viscosity of the treated effluent varied in the range 0.98–0.62 mPa·s which is approximately the same as the one for pure water (0.91–0.55 mPa·s).

3.3.2.1. Effect of transmembrane pressure

To determine the optimal operating pressure, filtration tests were carried out, at a temperature of 30°C, using different transmembrane pressures (TMP) ranging from 6 to 18 bar.

The evolution of the stabilized flux, obtained after 20 min of filtration, is illustrated in Fig. 7. It appears that there is a linear relationship between the permeate flux and the TMP that is established in the 6–10 bar pressure field. Beyond 10 bar, a deviation of the straight line is observed and the variation in the flux becomes negligible and then at high pressure values the permeate flux becomes constant. This behavior is attributed to the establishment of polarization concentration phenomena due to the accumulation of the retained substances on the membrane surface resulting in increase in the resistance to mass transport [66].

The characterization of the permeate obtained at each TMP shows total reduction in turbidity and SS whatever the used pressure while the retention of dissolved, organic and mineral pollutants increases with pressure up to 10 bar. The retention observed in terms of COD, salinity, chloride, sodium and sulfate are then approximately 85%, 62%, 38%, 65% and 83% respectively (Fig. 8). Beyond that, retention changes slightly and the performances in terms of permeate flux were limited by the concentration

Table 3
Principle physico-chemical characteristics of the textile wastewater

Parameter	Raw effluent	Rejection limit
pH	10	7 < pH < 8
Salinity (g/L)	15	–
Turbidity (NTU)	1,800	–
Color*	–	100
SS (mg/L)	509 ± 60	400
COD (mg/L)	2,700	1,000
Cl^- (mg/L)	1,580	700
Na^+ (mg/L)	1,980 ± 120	100
SO_4^{2-} (mg/L)	960 ± 100	500

*Integral of the absorbance curve in the whole visible range (400–800 nm).
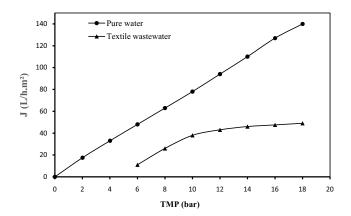

Fig. 7. Evolution of permeate flux of pure water and textile effluent with TMP.

polarization phenomenon. So, based on these results, 10 bar can be considered as the optimal TMP value.

3.3.2.2. Effect of salinity

The composition of textile wastewater effluent, especially coming from dye baths, generally varies from cycle to cycle depending on the amount of articles to be treated and also on the type of used dye and additives. In general, the quantity and the type of dyes vary according to the shade and the quality of the fabric which requires varied amounts of binding agents in terms of NaCl.

To study the effect of salt on the performance of NF membrane, the NaCl concentration in the effluent has been
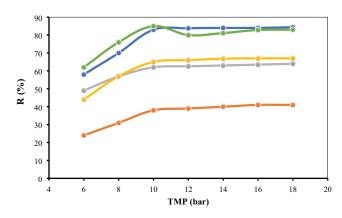
Fig. 8. Rejection of different soluble ions as a function of the TMP.

Fig. 9. Critical flux and rejection as a function of NaCl concentration.

modified from 3 to 17 g/L. The concept of critical flux was adopted in this case to explain the fouling. This approach consists of varying the pressure in the ascending then descending direction to determine then the steady flux to be achieved before proceeding to the next pressure [37,38]. According to this operating mode, inferior and superior limit values of the critical flux are determined. The critical flux has been defined as the first permeate flux for which irreversible fouling appears on the membrane surface.

Fig. 9 represents the evolution of critical flux and the performance of the permeate with the salt content. The increase of the salinity in the feed concentration up to 7 g/L results in a decrease in critical flux from 62 L/h m² (at 3 g/L) to 55 L/h m² (at 7 g/L). Beyond this value, the flux increases again and then stabilizes at 50 L/h m² from a salinity of 11 g/L. In addition, fouling becomes irreversible in the pressure interval 8–10 bar (critical pressure) regardless of the salinity used.

The evolution of the characteristics of the permeate shows a decrease in the retention of the different parameters (COD, Salinity, Chloride, Sodium) with the increase of NaCl concentration from 7 g/L. This behavior can be explained by the presence of electrostatic interactions between the effluent and the membrane [20,64,67]. When the concentration of NaCl is high, the electrostatic repulsion at the membrane surface is strong and eventually the salts pass easily through the membrane. On the other hand, a decrease in this concentration leads to an increase in rejection since strong electrostatic repulsion occurs at the active layer and therefore the salts are easily rejected.

From this result, it can therefore be considered easier to eliminate salts when their concentration in the treated solution is high, but this could be difficult when the concentration exceeds 13 g/L.

4. Conclusion

Microporous carbon membranes for nanofiltration have been successfully developed using phenolic resin as a precursor and source of carbon. The active layer of NF was deposited on the on the inner face of the MF supported membrane using the vacuum slip-casting process to uniform the distribution of the suspension on the entire inner
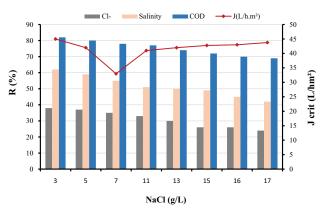
surface of the tube and to obtain a homogeneous and defect free layer in a single step.

Results show that it is possible to prepare a crack-free NF carbon membrane having a thickness of 1.36 μm, 1.1 nm average pore size and MWCO of 400 Da using 45% PR with a vacuum casting-time of 1min.

Performance of this membrane during the treatment of real textile wastewater has been studied in term of permeate flux and filtration efficiency. The best filtration performance was achieved at a TMP of 10 bar with a permeate flux of 13.5 L/h m². A total reduction in turbidity and SS, organic and mineral pollutants increases with pressure up to 10 bar. The retention observed in terms of COD, salinity, chloride, sodium and sulfate are then approximately 85%, 62%, 38%, 65% and 83% respectively.

This study revealed the combined process of biological sludge/NF carbon membranes was applied, not only to improve the rejection efficiencies, but also to recycle the permeate back into the dyeing process. In terms of economic benefit, the treated wastewater can be reused as refrigerating water, a washing water and a process water for the dyeing bath. For instance, water supply sources of textile factories are municipal water that costs 1.050 DT/1 m³ and a typical dye industry produces 400,000 m³of wastewater per year (which represents 35% of the region consumption). The volume of wastewater by such a company is large and highly colored with high loading of inorganic salt. Wastewater reuse is advisable, not only to reduce the environmental damage of the textile effluent, but also it offers an important economic benefit to the manufacturer since the cost of fresh water increases with consumption. The combined process of biological sludge/NF carbon membranes, as demonstrated in this study, will not only improve the treatment efficiency of the wastewater, but also provide clean water that could be used in the dyeing process.

The low rejection performance of NF in eliminating monovalent salts, especially NaCl, when treating highly salt-heavy effluents that exceed 7–11 g/L is an issue, but further optimization of the synthesis protocol for the membrane and process condition during the wastewater treatment could be instrumental to solving this problem [37,67]. Such a type of study shows that the NF carbon membrane

improves the quality of pretreated textile effluent allowing not only the reuse of the treated water but also the reduction of the quantity of salt to be added during the dyeing process.

Symbols

J_w	—	Water flux
L_w	—	Water permeability
R	—	Retention
R_m	—	Membrane resistance
R_{rev}	—	Reversible resistance
R_{irrev}	—	Irreversible resistance

References

[1] S. Yadav, H. Saleem, I. Ibrar, O. Naji, A.A. Hawari, A.A. Alanezi, S.J. Zaidi, A. Altaee, J. Zhou, Recent developments in forward osmosis membranes using carbon-based nanomaterials, Desalination, 482 (2020) 114375, doi: 10.1016/j.desal.2020.114375.

[2] N.U. Barambu, M.R. Bilad, M.A. Bustam, K.A. Kurnia, M.H.D. Othman, N.A.H.M. Nordin, Development of membrane material for oily wastewater treatment: a review, Ain. Shams. Eng. J., 12 (2021) 1361–1374.

[3] J. Mittal, Permissible synthetic food dyes in India, Resonance – J. Sci. Educ., 25 (2020) 567–577.

[4] A. Mittal, R. Ahmad, I. Hasan, Iron oxide-impregnated dextrin nanocomposite: synthesis and its application for the biosorption of Cr(VI) ions from aqueous solution, Desal. Water Treat., 57 (2015) 15133–15145.

[5] P. Saharan, V. Kumar, J. Mittal, V. Sharma, A.K. Sharma, Efficient ultrasonic assisted adsorption of organic pollutants employing bimetallic-carbon nanocomposites, Sep. Sci. Technol., 56 (2021) 2895–2908.

[6] P. Bernardo, E. Drioli, Membrane gas separation progresses for process intensification strategy in the petrochemical industry, Petrol. Chem., 50 (2010) 271–282.

[7] E. Drioli, A.I. Stankiewicz, F. Macedonio, Membrane engineering in process intensification-an overview, J. Membr. Sci., 380 (2011) 1–8, doi: 10.1016/j.memsci.2011.06.043.

[8] N.F. Himma, N. Prasetya, S. Anisah, I.G. Wenten, Superhydrophobic membrane: progress in preparation and its separation properties, Rev. Chem. Eng., 35 (2019) 211–238.

[9] N.F. Himma, A.K. Wardani, N. Prasetya, P.T.P. Aryanti, I.G. Wenten, Recent progress and challenges in membrane-based O_2/N_2 separation, Rev. Chem. Eng., (2018), doi: 10.1515/revce-2017-0094.

[10] I.G.B.N. Makertiharta, P.T. Dharmawijaya, I.G. Wenten, Current progress on zeolite membrane reactor for CO_2 hydrogenation, AIP Conf. Proc., 1788 (2018) 040001, doi: 10.1063/1.4968389.

[11] S. Abd Jalil, D.K. Wang, C. Yacou, J. Motuzas, S. Smart, J.C. Diniz da Costa, Vacuum-assisted tailoring of pore structures of phenolic resin derived carbon membranes, J. Membr. Sci., 525 (2018) 240–248.

[12] S. Alami-Younssi, A. Larbot, M. Persin, J. Sarrazin, L. Cot, Rejection of mineral salts on a gamma alumina nanofiltration membrane: application to environmental process, J. Membr. Sci., 102 (1995) 123–129.

[13] B.V. Der Bruggen, M. Mänttäri, M. Nyström, Drawbacks of applying nanofiltration and how to avoid them: a review, Sep. Purif. Technol., 63 (2008) 251–263.

[14] T.V. Gestel, C. Vandecasteelea, A. Buekenhoudt, C. Dotremont, J. Luyten, R. Leysen, B.V. Der Bruggen, G. Maes, Salt retention in nanofiltration with multilayer ceramic TiO_2 membranes, J. Membr. Sci., 209 (2002) 379–389.

[15] J.M. Gohil, R.R. Choudhury, Chapter 2 – Introduction to Nanostructured and Nano-Enhanced Polymeric Membranes: Preparation, Function, and Application for Water Purification, In: Nanoscale Materials in Water Purification, Nano and Micro Technologies, 2019, pp. 25–57. Available at: https://doi.org/10.1016/B978-0-12-813926-4.00038-0

[16] N. Hilal, H. Al-Zoubi, A.W. Mohammad, N.A. Darwish, Nanofiltration of highly concentrated salt solutions up to seawater salinity, Desalination, 184 (2005) 315–326.

[17] Y. Du, Y. Lv, W.-Z. Qiu, J. Wu, Z.-K. Xu, Nanofiltration membranes with narrowed pore size distribution via pore wall modification, Chem. Commun., 52 (2016) 8589–8592.

[18] M. Park, J. Park, E. Lee, J. Khim, J. Cho, Application of nanofiltration pretreatment to remove divalent ions for economical seawater reverse osmosis desalination, Desal. Water Treat., 57 (2016) 20661–20670.

[19] A.H. Hassani, R. Mirzayee, S. Nasseri, M. Borghei, M. Gholami, B. Torabifar, Nanofiltration process on dye removal from simulated textile wastewater, Int. J. Environ. Sci. Technol., 5 (2008) 401–408.

[20] E. Ellouze, N. Tahri, R. Ben Amar, Enhancement of textile wastewater treatment process using nanofiltration, Desalination, 286 (2012) 16–23.

[21] A.Y. Zahrim, C. Tizaoui, N. Hilal, Coagulation with polymers for nanofiltration pre-treatment of highly concentrated dyes: a review, Desalination, 266 (2011) 1–16.

[22] L. Shao, X.Q. Cheng, Y. Liu, S. Quan, J. Ma, S.Z. Zhao, K.Y. Wang, Newly developed nanofiltration (NF) composite membranes by interfacial polymerization for safranin O and aniline blue removal, J. Membr. Sci., 430 (2013) 96–105.

[23] A. Anand, A. Unnikrishnan, J.Y. Mao, H.J. Lina, C.C. Huang, Graphene-based nanofiltration membranes for improving salt rejection, water flux and antifouling–a review, Desalination, 429 (2018) 119–133.

[24] A.F. Ismail, L.I.B. David, A review on the latest development of carbon membranes for gas separation, J. Membr. Sci., 193 (2001) 1–18.

[25] M.M. Lorente-Ayza, S. Mestre, V. Sanz, E. Sanchez, On the underestimated effect of the starch ash on the characteristics of low-cost ceramic membranes, Ceram. Int., 42 (2016) 18944–18954.

[26] M. Lorente-Ayza, E. Sánchez, V. Sanz, S. Mestre, Influence of starch content on the properties of low-cost microfiltration ceramic membranes, Ceram. Int., 41 (2015) 13064–13073.

[27] H. Kaur, V.K. Bulasara, R.K. Gupta, Effect of carbonates composition on the permeation characteristics of low-cost ceramic membrane supports, J. Ind. Eng. Chem., 44 (2016) 185–194.

[28] I. Hedfi, N. Hamdi, M.A. Rodriguez, E. Srasra, Development of a low cost microporous ceramic membrane from kaolin and alumina, using the lignite as porogen agent, Ceram. Int., 42 (2016) 5089–5093.

[29] J. Yin, B. Deng, Polymer-matrix nanocomposite membranes for water treatment, J. Membr. Sci., 479 (2015) 256–275.

[30] M.O. Daramola, O.O. Sadare, O.O. Oluwasina, S.E. Iyuke, Synthesis and application of functionalized carbon nanotube infused polymer membrane (fCNT/PSF/PVA) for treatment of phenol-containing wastewater, J. Membr. Sci. Res., 5 (2019) 310–316.

[31] M.O. Daramola, B. Silinda, S. Masondo, O.O. Oluwasina, Polyether sulfone-sodalite (PES-SOD) mixed matrix membranes: prospect for acid mine drainage (AMD) treatment, J. S. Afr. I. Min. Metall., 115 (2015) 1221–1228.

[32] C.F. Unuigbe, O.M. Fayemiwo, M.O. Daramola, Performance evaluation of iron nanoparticles infused polyethersulphone (Fe-NPs/PES) membrane during treatment of BTEX-contaminated wastewater, Water Environ. J., 34 (2019) 74–86, doi: 10.1111/wej.12506.

[33] G. Baumgarten, D. Jakobs, H. Muller, Treatment of AOX-containing waste- water partial flows from pharmaceutical production processes with nanofiltration and reverse osmosis, Chem. Eng. Technol., 76 (2004) 321–325.

[34] A.R. Anim-Mensah, W.B. Krantz, R. Govind, Studies on polymeric nanofiltration-based water softening and the effect of anion properties on the softening process, Eur. Polym. J., 44 (2008) 2244–2252.

[35] S. Ghizellaoui, A. Chibani, S. Ghizellaoui, Use of nanofiltration for partial softening of very hard water, Desalination, 179 (2005) 315–322.

[36] C. Li, C. Song, P. Tao, M. Sun, Z. Pan, T. Wang, M. Shao, Enhanced separation performance of coal-based carbon membranes coupled with an electric field for oily wastewater treatment, Sep. Purif. Technol., 168 (2016) 47–56.

[37] N. Tahri, I. Jedidi, S. Cerneaux, M. Cretin, R. Ben Amar, Development of an asymmetric carbon microfiltration membrane: application to the treatment of industrial textile wastewater, Sep. Purif. Technol., 118 (2013) 179–187.

[38] N. Tahri, I. Jedidi, S. Ayadi, S. Cerneaux, M. Cretin, R. Ben Amar, Preparation of an asymmetric microporous carbon membrane for ultrafiltration separation: application to the treatment of industrial dyeing effluent, Desal. Water Treat., 57 (2016) 23473–23488, doi: 10.1080/19443994.2015.1135826.

[39] C. Song, T. Wang, Y. Pan, J. Qiu, Preparation of coal based microfiltration carbon membrane and application in oily wastewater treatment, Sep. Purif. Technol., 51 (2006) 80–84.

[40] C. Song, T. Wang, J. Qiu, Y. Cao, T. Cai, Effects of carbonization conditions on the properties of coal-based microfiltration carbon membranes, J. Porous Mater., 15 (2008) 1–6.

[41] Z. Chen, F. Chen, F. Zeng, J. Li, Preparation and characterization of the charged PDMC/Al_2O_3 composite nanofiltration membrane, Desalination, 349 (2014) 106–114.

[42] C.M. Wu, T.W. Xu, W.H. Yang, Fundamental studies of a new hybrid (inorganic–organic) positively charged membrane: membrane preparation and characterizations, J. Membr. Sci., 216 (2003) 269–278.

[43] J. Xiao, C. Xiong, L. Ding, H. Yuan, L. Chen, W. Liu, Tubular solid oxide fuel cells fabricated by slip-phase inversion combined with a vacuum-assisted coating technique, Ceram. Int., 40 (2014) 10163–10169.

[44] T.A. Centeno, J.L. Vilas, A.B. Fuertes, Effects of phenolic resin pyrolysis conditions on carbon membrane performance for gas separation, J. Membr. Sci., 228 (2004) 45–54.

[45] M. Teixeira, M. Campo, D.A. Tanaka, M.A. Tanco, C. Magen, A. Mendes, Carbon Al_2O_3 Ag composite molecular sieve membranes for gas separation, Chem. Eng. Res. Des., 90 (2012) 2338–2345.

[46] M. Teixeira, M.C. Campo, D.A. Tanaka, M.A. Tanco, C. Magen, A. Mendes, Composite phenolic resin-based carbon molecular sieve membranes for gas separation, Carbon, 49 (2011) 4348–4358.

[47] X.L. Pan, N. Stroh, H. Brunner, G.X. Xiong, S.S. Sheng, Deposition of sol–gel derived membranes on Al_2O_3 hollow fibers by a vacuum-assisted dip-coating process, J. Membr. Sci., 226 (2003) 111–118.

[48] A.B. Fuertes, T.A. Centeno, Preparation of supported asymmetric carbon molecular sieve membranes, J. Membr. Sci., 144 (1998) 105–111.

[49] L. Li, C. Song, H. Jiang, J. Qiu, T. Wang, Preparation and gas separation performance of supported carbon membranes with ordered mesoporous carbon interlayer, J. Membr. Sci., 450 (2014) 469–477.

[50] M.A. Anderson, M.J. Gieselmann, Q.Y. Xu, Titania and alumina ceramic membranes, J. Membr. Sci., 39 (1988) 243–258.

[51] M. Mahdyarfar, T. Mohammadi, A. Mohajeri, Gas separation performance of carbon materials produced from phenolic resin: effects of carbonization temperature and ozone post treatment, New Carbon Mater., 28 (2013) 39–46.

[52] H. Kita, H. Maeda, K. Tanaka, K. Okamoto, Carbon molecular sieve membrane prepared from phenolic resin, Chem. Lett., 26 (1997) 179–180.

[53] T.A. Centeno, A.B. Fuertes, Carbon molecular sieve membranes derived from a phenolic resin supported on porous ceramic tubes, Sep. Purif. Technol., 25 (2001) 379–384.

[54] K. Briceno, D. Montané, R. Garcia-Valls, A. Iulianelli, A. Basile, Fabrication variables affecting the structure and properties of supported carbon molecular sieve membranes for hydrogen separation, J. Membr. Sci., 415–416 (2012) 288–297.

[55] M.A. Llosa-Tanco, D.A. Pacheco Tanaka, A Mendes, Composite-alumina-carbon molecular sieve membranes prepared from novolac resin and boehmite, Part II: Effect of the carbonization temperature on the gas permeation properties, Int. J. Hydrogen Energy, 40 (2014) 3485–3496.

[56] S.C. Rodrigues, R. Whitley, A. Mendes, Preparation and characterization of carbon molecular sieve membranes based on resorcinol–formaldehyde resin, J. Membr. Sci., 459 (2014) 207–216.

[57] A. Margot. L. Tanco, D.A. Pacheco Tanaka, Ad_elio Mendes, Composite-alumina-carbon molecular sieve membranes prepared from novolac resin and boehmite. Part II: Effect of the carbonization temperature on the gas permeation properties, Int. J. Hydrogen Energy, 40 (2015) 3485–3496.

[58] N.H. Ismail, W.N.W. Salleh, N. Sazali, A.F. Ismail, N. Yusof, F. Aziz, Disk supported carbon membrane via spray coating method: Effect of carbonization temperature and atmosphere, Sep. Purif. Technol., 195 (2018) 295–304.

[59] T.A. Centeno, A.B. Fuertes, supported carbon molecular sieve membranes based on a phenolic resin, J. Membr. Sci., 160 (1999) 201–211.

[60] S. Otani, A. Oya, In: R.W. Cahn, P. Haasen, E.J. Kramer, Eds., Materials Science and Technology: A Comprehensive Treatment, Vol. 9, VCH, Weinheim, 1991, p. 559.

[61] K. Miura, J. Hayashi, K. Hashimoto, Production of molecular sieving carbon through carbonization of coal modified by organic additives, Carbon, 29 (1991) 653–660.

[62] T.H. Ko, W.S. Kuo, Y.H. Chang, Raman study of the microstructure changes of phenolic resin during pyrolysis, Polym. Compos., 21 (2000) 745–750.

[63] C. Allègre, P. Moulin, M. Maisseu, F. Charbit, Treatment and reuse of reactive dyeing effluents, J. Membr. Sci., 269 (2006) 15–34.

[64] B. Van der Bruggen, B. Daems, D. Wilms, C. Vandecasteele, Mechanisms of retention and flux decline for the nanofiltration of dye baths from the textile industry, Sep. Purif. Technol., 22 (2001) 519–528.

[65] B. Van der Bruggen, G. Cornelis, C. Vandecasteele, I. Devreese, fouling of nanofiltration and ultrafiltration membranes applied for wastewater regeneration in the textile industry, Desalination, 175 (2005) 111–119.

[66] Q. Chen, Y. Yang, M. Zhou, M. Liu, S. Yu, C. Gao, Comparative study on the treatment of raw and biologically treated textile effluents through submerged nanofiltration, J. Hazard. Mater., 284 (2015) 121–129.

[67] N. Tahri, G. Masmoudi, E. Ellouze, A. Jrad, P. Drogui, R. Ben Amar, coupling microfiltration and nanofiltration processes for the treatment at source of dyeing-containing effluent, J. Cleaner Prod., 33 (2012) 226–235.